Inorganic Chemistry

Article

pubs.acs.org/IC

Introduction of Lewis Acidic and Redox-Active Sites into a Porous Framework for Ammonia Capture with Visual Color Response

Bin Tan,[†] Cheng Chen,[†] Li-Xuan Cai,[†] Ya-Jun Zhang,[†] Xiao-Ying Huang,[†] and Jie Zhang*[,†,‡]

[†]State Key Laboratory of Structural Chemistry, Fujian Institute of Research on the Structure of Matter, Chinese Academy of Sciences, Fuzhou, Fujian 350002, People's Republic of China

[‡]School of Chemistry, Beijing Institute of Technology, Beijing, 100081, People's Republic of China

Supporting Information

ABSTRACT: Based on the Lewis acidic site and redox ability of bipyridinium ligand, a porous framework with an adsorption advantage for ammonia over water and color response ability has been constructed. The compound is highly stable and flexible to external stimuli, exhibiting reversible single-crystal-to-single-crystal transformations, in response to temperature change and NH_3 capture. More attractively, the title compound shows obvious color change from yellow to dark blue when exposed to ammonia vapor within just a few seconds, indicating a strong ability to function as a visual colorimetric absorbent for ammonia.

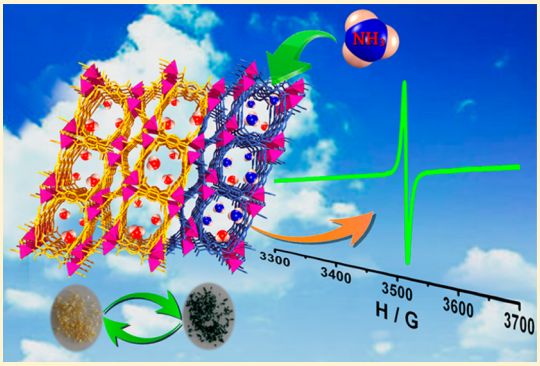

INTRODUCTION

Ammonia is ubiquitous in nature as an end product of protein metabolism and has been widely used in food, fertilizer, dyeing, and refrigeration equipment production industries. However, it is toxic, corrosive, and difficult to handle, and can be easily absorbed through the skin to endanger life safety when leaked out, even in very low concentration. Besides, it can lead to the formation of a secondary particulate matter in the atmosphere that affects atmospheric visibility and global radiation balance.[1] For the concerns about environment safety and human health, it is extremely significant to explore new materials for capturing and sensing ammonia pollutant. Porous metal−organic framework (MOF) materials possess strong advantages in providing designable interaction sites for achieving target specific adsorption.[2] To date, some progress has been made in generating ammonia adsorbents,[3−9] such as Cu-PCP (MOF-199),[3] MOF-5 and MOF-177,[4] DUT-6 (MOF-205) and Zn-MOF,[5] zirconium-based UiO-66,[6] as well as the related materials known as covalent organic frameworks COF-10[7] and BPP-5.[8] However, problems emerge in the development of the related MOF materials:

(1) Because of the interactions between adsorbate and the open metal sites or organic groups that are responsible for the enhanced adsorption capability, the adsorption process commonly is irreversible, or structural collapse may occur during adsorption of ammonia,[3−5] which destroys their application potential.
(2) The competitive adsorption of water extensively exists because of the omnipresence of moisture and the common attribute of two molecules in polarity, coordination, and hydrogen bonding ability. For practical application, it is strongly desirable to develop effective approaches to construct stable and recyclable materials for ammonia capture that are immune to the negative influence of moisture.

Viologen/bipyridinium derivatives possess excellent redox ability and can act as good electron acceptors (Lewis acidic sites) to apply in different fields.[10] Upon one-electron reduction to produce intensely colored free radicals, obvious color changes can be observed for these compounds.[11] Since ammonia is a Lewis base and a reducing agent, the functionalization of pore surface by introducing such organic molecules into framework materials not only may enhance the adsorption selectivity/efficiency toward ammonia molecules via acid−base interaction, but also likely induces a color change in response to guest adsorption. More importantly, the pyridinium functional moiety has no hydrogen bonding sites, which is advantageous for eliminating the competitive adsorption of water (Figure 1). Along these lines, herein, a bipyridinium salt, 1,1′-[1,4-phenylene-bis(methylene)]bis(4,4′-bipyridinium) dichloride ($\mathbf{L}\cdot Cl_2$), was synthesized and used to construct a unique Zn-based MOF, called $[Zn_2(\mathbf{L})(PMC)_{1.5}]\cdot 12H_2O$ (**1**, H_4PMC = pyromellitic acid). Compound **1** features a non-interpenetrated two-dimensional (2D) network with a one-dimensional (1D) channel. As expected, **1** shows a good NH_3 adsorption ability and can undergo significant color change from yellow to dark blue when exposing to NH_3 vapor, which

Received: January 5, 2015
Published: March 11, 2015

DOI: 10.1021/acs.inorgchem.5b00023
Inorg. Chem. 2015, 54, 3456−3461

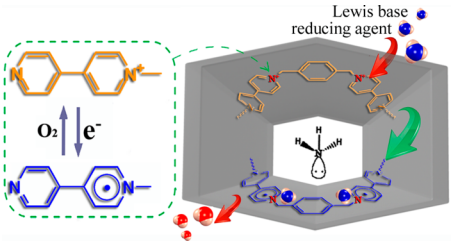

Figure 1. Strategy for ammonia adsorption with visual color response.

represents the first example as a visual colorimetric capture and sensing framework materials for NH_3 in reversible process. Attractively, a direct replacement of water by NH_3 in channel can be observed and occurs in a reversible single-crystal-to-single-crystal (SC-SC) transformation, providing a valuable insight into the exploration of ammonia capture and sensing materials.

EXPERIMENTAL SECTION

Materials and Physical Measurements. All chemical reagents were obtained from commercial sources and used as received. Elemental analyses (EA) of C, H, and N were performed on a Vario EL III CHNOS elemental analyzer. Powder X-ray diffraction (PXRD) patterns were recorded in the angular range of $2\theta = 5°-65°$ with a scan speed of 1° min^{-1} on a Rigaku MiniFlex II diffractometer using Cu Kα radiation. Variable-temperature PXRD patterns were recorded on a Rigaku D/MAX2500 diffractometer using Cu Kα radiation with a scan speed of 5° min^{-1} in the angular range of $2\theta = 5°-55°$ from 30 °C to 130 °C. The infrared spectra were taken on a Bomem MB-102 IR spectrometer with samples as KBr pellets in the range of 4000−400 cm^{-1}. UV-vis diffuse reflectance spectra were measured using a Perkin−Elmer Model Lambda 950 spectrometer, with a $BaSO_4$ plate as a standard (100% reflectance). Electron spin resonance (ESR) signals were recorded with a Bruker Model A300 spectrometer. Thermogravimetric analysis (TGA) was carried out with a Mettler Model TGA/SDTA851^e thermal analyzer at a heating rate of 10 °C min^{-1} under an atmosphere of flowing air on the pure powder samples from 30 °C to 800 °C. Thermogravimetric analysis−mass spectroscopy (TGA-MS) was performed on a Netzsch Model STA449C-QMS 403 C unit at a heating rate of 10 °C min^{-1} under a nitrogen atmosphere. N_2 sorption isotherm, BET, and Langmuir surface areas were measured on the Accelerated Surface Area and Porosimetry (ASAP) 2020 System; the sample was degassed at 25 °C for 1 h prior to the measurements being taken.

Synthesis of L·Cl_2. 1,1′-[1,4-Phenylenebis(methylene)]bis-(4,4′-bipyridinium) dichloride (**L**·Cl_2) was synthesized based on the nucleophilic substitution reaction of 4,4′-bipyridine and 1,4-bis(chloromethyl)benzene (see Scheme S1 in the Supporting Information). A mixture of 4,4′-bipyridine (2.343 g, 15 mmol) and 1,4-bis(chloromethyl)benzene (0.882 g, 5 mmol) was dissolved in 20 mL of *N*,*N*′-dimethylformamide (DMF) and then stirred at 110 °C for 6 h. The resulting yellow precipitate was collected by filtration under hot conditions, washed with hot DMF solution, and air-dried to give **L**·Cl_2 as a yellow powder (85% yield).

Synthesis of 1. A mixture of **L**·Cl_2 (0.1 mmol, 0.049 g), H_4PMC (pyromellitic acid, 0.1 mmol, 0.025 g), $ZnSO_4$ solution (2 mL, 0.5 mol L^{-1}) and DMF (3 mL) stirred for 20 min, then sealed in a 20 mL vial and kept at 110 °C for 40 h. The yellow laminar-like crystals of **1** were collected by filtration and washed with distilled water after the vial cooled to room temperature (yield: 0.064 g, 56% based on **L**·Cl_2).

X-ray Crystallography. Data collection were performed on an Agilent Diffraction SuperNova dual diffractometer, with Cu Kα radiation (λ = 1.54178 Å) at 293 K for **1**, 100 K for **1-L**, and **1-NH_3**. Absorption corrections were performed using a multi-

Table 1. Crystallographic Data for 1, 1-L, and 1-NH_3

	1	1-L	1-NH_3
empirical formula	$C_{43}H_{51}N_4O_{24}Zn_2$	$C_{43}H_{51}N_4O_{24}Zn_2$	$C_{43}H_{57}N_8O_{21}Zn_2$
formula weight	1138.62	1138.62	1152.71
crystal system	monoclinic	monoclinic	monoclinic
space group	*I*2/*m*	$P2_1/n$	$P2_1/n$
temperature, *T* (K)	293	100	100
wavelength, λ (Å)	1.54178	1.54178	1.54178
a (Å)	11.3404(2)	11.12310(10)	11.3257(4)
b (Å)	29.1741(7)	29.0062(4)	29.3273(13)
c (Å)	14.8727(3)	14.7756(2)	14.7879(7)
β (deg)	92.023(2)	91.5430(10)	91.693(3)
V (Å^3)	4917.51(18)	4765. 45(10)	4909.7(4)
Z	4	4	4
μ (mm^{-1})	1.990	2.054	1.976
F(000)	2356	2356	2396
No. of reflections measured	9519	20 186	17 846
No. of independent reflections	4763	9491	8655
ρ_{calc} (g cm^{-3})	1.538	1.587	1.559
No. of parameters	337	742	740
R_{int}	0.0205	0.0193	0.0384
R_1, wR_2 $[I > 2\sigma(I)]^{a,b}$	0.0512, 0.1205	0.0464, 0.1327	0.1241, 0.2483
goodness of fit, GOF	1.017	1.007	1.037
largest diff. peak and hole/e Å^{-3}	0.312, −0.362	0.607, −0.482	1.887, −1.422

$^aR_1 = \sum||F_0| - |F_c||/\sum|F_0|$. $^bwR_2 = [\sum w(F_0^2 - F_c^2)^2/\sum w(F_0^2)^2]^{1/2}$.

DOI: 10.1021/acs.inorgchem.5b00023
Inorg. Chem. 2015, 54, 3456−3461

scan method. The structures were solved by direct methods and refined by full-matrix least-squares on F^2 using the SHELX-97 program package.[12] All of the non-hydrogen atoms were refined anisotropically. H atoms attached to the C, O atoms were located by geometrical calculations, and their positions and thermal parameters were fixed during structural refinement. In **1**, some constraints (SIMU, DFIX, SADI, and DANG) were applied to the H_2O molecules and the disordered parts of pyridine ring of the **L** ligand. In **1-L**, some constraints (SIMU, DFIX, and DANG) were applied to the H_2O molecules. In **1-NH$_3$**, some constraints (SADI and SIMU) were applied to the disordered parts of pyridine ring of the ligand **L**. It was difficult to locate all of the disordered H_2O and NH_3 molecules based on the difference-Fourier maps of compounds **1**, **1-L**, and **1-NH$_3$**. Therefore, finally, only partial lattice water molecules were assigned and refined and the remaining H_2O and NH_3 molecules were based on the elemental analyses. The empirical formulas were confirmed by the element analysis (EA) results. The relevant crystallographic data and structural refinement details are listed in Table 1.

RESULTS AND DISCUSSION

Crystal Structure Description. Compound **1** was obtained when a mixture of **L**·Cl_2, H_4PMC, $ZnSO_4$ solution, and DMF was sealed and heated at 110 °C for 40 h. Single-crystal X-ray diffraction (XRD) analysis indicates that **1** crystallizes in the monoclinic crystal system, space group *I*2/*m*. The asymmetric unit contains one crystallographically independent Zn^{2+} ion, half of **L** molecule mirrored symmetrically along the center line of the benzene ring, and three-quarters of PMC^{4-} ligands (see Figure S1 in the Supporting Information). Each Zn^{2+} ion is tetrahedrally coordinated by three carboxylate O atoms from three PMC^{4-} ligands in a monodentate fashion and one N atom from an **L** ligand. Then two Zn^{2+} ions are bridged by three PMC^{4-} ligands by a pair of carboxyl (COO^-) groups in the ortho-position to form a dimer. Consequently, each PMC^{4-} ligand links four Zn^{2+} ions of two dimers through four COO^- groups. Thus, the dimer can be regarded as a three-way node to be connected to three neighboring dimers to form an anionic honeycomb-like 2D (6,3) network that contains large edge-sharing planar hexagonal rings with the dimers acting as corners and the PMC^{4-} ligands as edges. On and beneath the planar hexagonal ring, each flexible **L** ligand adopting *cis* configurations is linked to two Zn atoms from two different neighboring dimers (Figure 2a), which neutralizes the (6,3) network and gives rise to a concavo-convex layer with 1D trapezia-shaped channels parallel to the (6,3) network. The adjacent layers are stacked in an AB sequence along the [101] direction in a non-interpenetrating mode (see Figure S2 in the Supporting Information), and the **L** ligands are inserted into the hexagonal rings. Consequently, the large 1D hexagonal channel with a pore size of 16.84 Å × 16.84 Å (the distances have been measured between the carboxyl O atoms located on the diagonal) along the *c*-axis was formed as described in Figure 2b. Calculations using the PLATON program[13] show that the total solvent accessible volume is ~27.6% after removing all H_2O molecules. The N_2 sorption at 77 K revealed a Type-I sorption behavior (Figure 3) with small

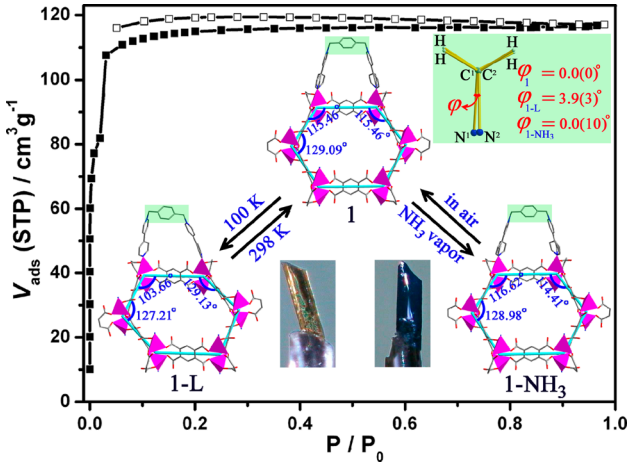

Figure 2. (a) The two-dimensional (2D) plane viewed along the *a*-axis. (b) The one-dimensional (1D) channels viewed along the *c*-axis. The guest species, the disordered parts of pyridine ring, and all H atoms are omitted for clarity. The magenta polyhedron represents Zn tetrahedral geometry.

Figure 3. N_2 sorption isotherm of **1** at 77 K. The inset shows a view of the planar hexagonal ring and **L** ligand in the 2D honeycomb layer for compounds **1** (top), **1-L** (left) and **1-NH$_3$** (right); the diagram of N^1–C^1···N^2–C^2 and the value of φ located on the upper left corner; the photographs of crystals **1-L** (left) and **1-NH$_3$** (right) are also shown.

hysteresis. The N_2 uptake around 1 atm is ~117 $cm^3\ g^{-1}$, with BET and Langmuir surface areas of 367.1 $m^2\ g^{-1}$ and 509.0 $m^2\ g^{-1}$, respectively. It is interesting to note that the isotherm shows an abrupt increase at point P/P_0 = 0.02, indicating that structural transformation is probably involved during the nitrogen adsorption process.[14]

Structure Transformations. To evaluate the structural flexibility of the title compound, the single-crystal diffraction data of **1** under low temperature was further collected. It was found that **1** at 100 K (**1-L**) exhibited the same yellow laminar-like appearance as **1**. However, a reversible SC-SC transformation occurred between them. Compound **1-L** belongs to the $P2_1/n$ space group, and has the double asymmetric unit contents (see Figure S3 in the Supporting Information). Under 100 K, the flexible **L** ligand in **1-L** undergoes some torsional motion, leading to a synclinal alignment of two bipyridinium groups (see Figure 3). The torsion angle φ, which is defined by three bond vectors (involving the terminal pyridine N^1 to one methylene C^1, the C^1 to another methylene C^2, and the C^2 to another terminal pyridine N^2), changes from 0.0(0)° to 3.9(3)°. Accordingly, the large hexagonal ring also undergoes alteration from an almost perfect one to a compressed one, with the interior angles changing from 115.46°–129.09° in **1** to 103.66°–129.13° in **1-L**. The total solvent-accessible volume decreased to 26.9% after removing all the free water molecules. These results clearly reveal the ability of the title compound to expand or shrink, in response to external stimuli.

Remarkably, when exposed to NH_3 vapor or pure NH_3 gas for several seconds, the yellow crystal of **1** immediately gave a

DOI: 10.1021/acs.inorgchem.5b00023
Inorg. Chem. 2015, 54, 3456–3461

color change to dark blue that was detectable by the naked eye (**1-NH$_3$**, inset of Figure 3). Most importantly, **1-NH$_3$** still retained its single-crystal nature and the crystal data of **1-NH$_3$** was collected at 100 K (see Figure S4 in the Supporting Information). Single-crystal analysis revealed that a guest-induced SC-SC phase transition occurred during the ammonia adsorption process. Compared to **1-L**, because of the interactions between NH_3 molecule (electron donor) and the **L** ligand (electron acceptor), the spatial orientation of the two bipyridinium groups tends to be in eclipsed form, the torsion angle φ decreases from 3.9(3)° to 0.0(10)°, approaching that observed in **1**. Sequentially, the hexagonal ring also becomes expanding, with interior angles ranging from 114.41° to 128.98° (see Figure 3). The total solvent-accessible volume reaches 27.9% after removal of the guest molecules. These data further demonstrate that the title compound possesses high stability and flexibility to respond to the adsorption of guest ammonia molecules.

Ammonia Adsorption and Color Response Behavior. To explore the color change mechanism, the solid UV-vis diffuse reflectance spectra of **L**·Cl_2, samples for **1**, **1-NH$_3$**, and **1-NH$_3$′** (**1-NH$_3$** placed in air for several hours) were measured. As shown in Figure 4, the new absorption band with a maximum at 620 nm appears in the spectrum of **1-NH$_3$**. Such a characteristic absorption band is similar to that of the free radicals generating from the bipyridinium derivatives through photoinduced electron transfer,[10,11] suggesting that the ammonia-induced color change is likely to arise from the generation of the bipyridinium radicals. This radical generation can be further confirmed by the electron spin resonance (ESR) spectral analysis. After exposure to NH_3 vapor for a while and further extending that period to 1.5 h, the sample exhibited a strong ESR signal at g = 2.0029 (see Figure 5) with increasing exposure time, which is similar to those found in photoinduced bipyridinium derivatives.[11,15] Besides, the IR spectra also provide a direct evidence for the adsorption of ammonia molecules and the simultaneous generation of radicals (see the inset of Figure 4). The appearance of weak broad bands around 3334 cm^{-1}, which corresponds to the ν_{N-H}, is indicative of the existence of ammonia. While a new vibration band at ca. 1637 cm^{-1} (highlighted in blue star) can be assigned to the C═N stretching vibration of the pyridinium ring in the **L**$^{\bullet}$ free-radical ligand, since the generation of the free radicals increases the electron density of the C═N double bond and, thus, can cause the blue-shift of stretching frequency. The above results indicate that, when sample **1** was exposed to NH_3 vapor, the ammonia molecules may act as an electron donor to donate electrons to the **L** ligand to generate **L**$^{\bullet}$ free radicals and are accompanied by an obvious visual color change. After leaving **1-NH$_3$** in air for several hours, the 620 nm absorption band became weaker and ultimately disappeared (see Figure 4). The visible change was that the dark blue color returned to the initial yellow, because of the quenching of the free radicals under an air atmosphere through a process of oxidation from **L**$^{\bullet}$ to **L** by O_2 in air,[10d] indicating the colorimetric reversibility of the title compound.

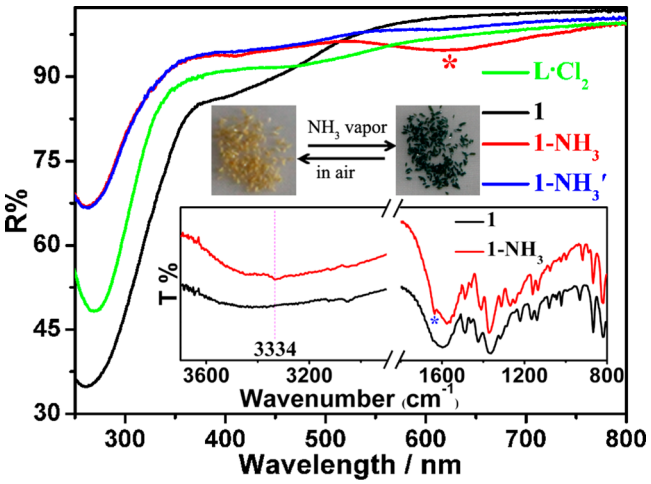

Figure 4. UV-vis diffuse reflectance spectra of **L**·Cl_2, **1**, **1-NH$_3$**, and **1-NH$_3$′**. The inset shows IR spectra of compounds **1** and **1-NH$_3$**. The characteristic spectral band, denoted by an asterisk (*), represents the sign of the viologen radical. The photographs show the color change of **1** before and after being exposed to NH_3 vapor.

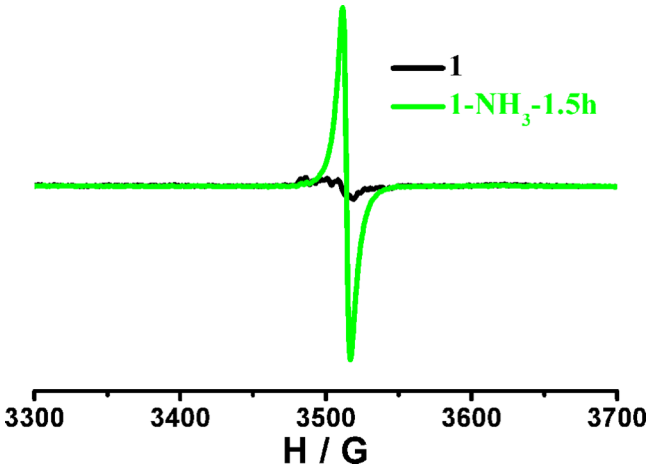

Figure 5. ESR spectra of **1** and **1** exposed to NH_3 vapor in the solid state at room temperature. The very weak ESR signal observed for **1** should arise from an ambient light-induced radical generation due to the photoactivity of **1**.

During the NH_3-triggered color evolution, except the bipyridinium radicals, no new species related to NH_3 can be detected in the framework, which may be due to the fact that the oxidation of NH_3 gives a product with low molecular weight and volatile properties may be difficult to be detected (e.g., N_2).[16] Simultaneous thermogravimetric and mass spectrometric (TGA-MS) analysis revealed that the detectable species evolved from TGA only contain NH_3 and H_2O molecules during a weight transition (see Figure S5 in the Supporting Information). In addition, the 1430 cm^{-1} band assigned to the vibration of N−H in NH_4^+ does not emerge in the IR spectrum of **1-NH$_3$**,[3c,17] excluding the possibility that NH_3 molecules interact with guest water molecules to form new species, such as NH_4^+.[3b]

The NH_3 contents and the reversible SC-SC phase transition can be further determined by element analysis (see Figure 6 and Table S1 in the Supporting Information) and PXRD (see Figure S6 in the Supporting Information). Variable-temperature PXRD data for **1** were measured from 30 °C to 130 °C (see Figure S7 in the Supporting Information) for further determining the stability of the title compound. From 30 °C to 120 °C, no obvious changes in the PXRD patterns indicated that the framework of **1** can be stable to 120 °C. When **1** was activated at 110 °C for 6 h, the empirical formula of **1** changed from $[Zn_2(\mathbf{L})(PMC)_{1.5}]\cdot 12H_2O$ to $[Zn_2(\mathbf{L})(PMC)_{1.5}]\cdot 1.5H_2O$.

DOI: 10.1021/acs.inorgchem.5b00023
Inorg. Chem. 2015, 54, 3456−3461

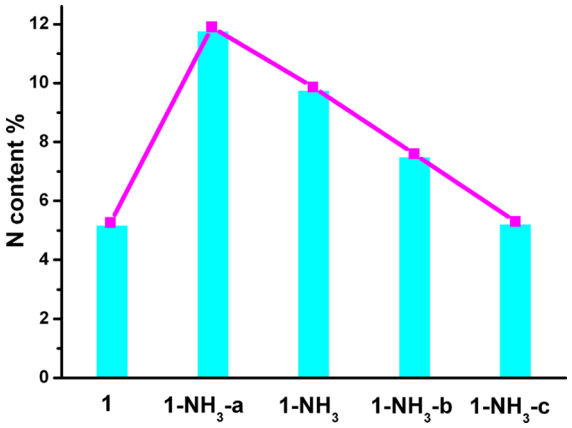

Figure 6. Column graph representing the variation of N contents in compounds **1** before and after ammonia adsorption.

The activated sample was exposed to ammonia vapor (humid) for a while, then a color change to dark blue occurred and gave a sample that was labeled as **1-NH$_3$-a**, which exhibits the empirical formula of $[Zn_2(\mathbf{L})(PMC)_{1.5}]\cdot 7.75H_2O\cdot 5.75NH_3$. The NH_3 capture capacity was ~5.0 mol kg^{-1}, based on the activated $[Zn_2(\mathbf{L})(PMC)_{1.5}]\cdot 1.5H_2O$. The ammonia absorption value was comparable to the capacities of the traditional adsorbents, such as alumina, silica gel, and activated carbon (2.2−5.3 mol kg^{-1}), as well as 5.1 mol kg^{-1} for Cu-PCP (MOF-199),[3a,18] despite the fact that the pore volume of **1** (0.18 cm^3 g^{-1}) was much smaller than that of MOF-199 (0.75 cm^3 g^{-1}), suggesting a high ammonia-accepting ability of the title compound. Actually, when the as-synthesized sample without any heat treatment was directly exposed to ammonia vapor (humid) for 10 min, the empirical formula changed to $[Zn_2(\mathbf{L})(PMC)_{1.5}]\cdot 9H_2O\cdot 4NH_3$, namely **1-NH$_3$**. This NH_3 capture ability was close to the activated one, indicating a strong affinity between the framework and guest NH_3 molecules, which resulted in a direct replacement of water molecules by NH_3. Upon leaving **1-NH$_3$** in air for several hours, the content of NH_3 molecules decreased from four per molecular formula to two per molecular formula, marked as **1-NH$_3$-b**; this compound was light blue and its empirical formula was $[Zn_2(\mathbf{L})(PMC)_{1.5}]\cdot 9H_2O\cdot 2NH_3$. When **1-NH$_3$-b** crystals continuously placed in air for several days, the light blue sample could be returned to the initial yellow crystals named as **1-NH$_3$-c**, with the empirical formula of $[Zn_2(\mathbf{L})(PMC)1.5]\cdot 12H_2O$. The reported MOF materials with high ammonia absorption ability were based on the acid−base interactions between NH_3 molecule and the open metal sites or organic groups of the coordination frameworks, but generally suffered the structural collapse that limited the application.[3−5] Benefitted from the unique character of the bipyridinium **L** ligand to act as a good electron acceptor for NH_3 (an electron donor), compound **1** could be utilized as a recyclable storage material and visual colorimetric sensor for NH_3.

CONCLUSIONS

In summary, based on a bipyridinium derivative with Lewis acidic site and high redox activity, a unique porous framework with recyclable adsorption and visual color response for NH_3 has been developed. The title compound undergoes a direct replacement of water molecules by NH_3 accompanied by an obvious visible color change from yellow to dark blue, and exhibits an interesting reversible single-crystal-to-single-crystal (SC-SC) phase transformations under the different temperatures and NH_3 environment. This work provides a new way to design framework materials with guest-responsive naked-eye colorimetric properties as convenient capture and practical sensing materials for environment pollutants.

ASSOCIATED CONTENT

Supporting Information

Additional figures and tables. This material is available free of charge via the Internet at http://pubs.acs.org. CCDC Nos. 1027488−1027490 for **1**, **1-L**, and **1-NH$_3$**.

AUTHOR INFORMATION

Corresponding Author

*E-mail: zhangjie@fjirsm.ac.cn.

Notes

The authors declare no competing financial interest.

ACKNOWLEDGMENTS

This work was supported by the grants from the NNSF of China (Grant Nos. 21271173/20973171).

REFERENCES

(1) Bashkova, S.; Bandosz, T. J. *J. Colloid Interface Sci.* **2014**, *417*, 109−114.

(2) (a) Chen, B. L.; Xiang, S. C.; Qian, G. D. *Acc. Chem. Res.* **2010**, *43*, 1115−1124. (b) Sumida, K.; Rogow, D. L.; Mason, J. A.; McDonald, T. M.; Bloch, E. D.; Herm, Z. R.; Bae, T.-H.; Long, J. R. *Chem. Rev.* **2012**, *112*, 724−781. (c) Barea, E.; Montoro, C.; Navarro, J. A. R. *Chem. Soc. Rev.* **2014**, *43*, 5419−5430. (d) Almeida Paz, F. A.; Klinowski, J.; Vilela, S. M. F.; Tomé, J. P. C.; Cavaleiro, J. A. S.; Rocha, J. *Chem. Soc. Rev.* **2012**, *42*, 1088−1110. (e) Cohen, S. M. *Chem. Rev.* **2012**, *112*, 970−1000.

(3) (a) Britt, D.; Tranchemontagne, D.; Yaghi, O. M. *Proc. Natl. Acad. Sci. U. S. A.* **2008**, *105*, 11623−11627. (b) Peterson, G. W.; Wagner, G. W.; Balboa, A.; Mahle, J.; Sewell, T.; Karwacki, C. J. *J. Phys. Chem. C* **2009**, *113*, 13906−13917. (c) Petit, C.; Mendoza, B.; Bandosz, T. J. *Langmuir* **2010**, *26*, 15302−15309. (d) Petit, C.; Huang, L. L.; Jagiello, J.; Kenvin, J.; Gubbins, K. E.; Bandosz, T. J. *Langmuir* **2011**, *27*, 13043−13051.

(4) Saha, D.; Deng, S. G. *J. Colloid Interface Sci.* **2010**, *348*, 615−620.

(5) Spanopoulos, I.; Xydias, P.; Malliakas, C. D.; Trikalitis, P. N. *Inorg. Chem.* **2013**, *52*, 855−862.

(6) (a) Cavka, J. H.; Jakobsen, S.; Olsbye, U.; Guillou, N.; Lamberti, C.; Bordiga, S.; Lillerud, K. P. *J. Am. Chem. Soc.* **2008**, *130*, 13850−13851. (b) Morris, W.; Doonan, C. J.; Yaghi, O. M. *Inorg. Chem.* **2011**, *50*, 6853−6855.

(7) Doonan, C. J.; Tranchemontagne, D. J.; Glover, T. G.; Hunt, J. R.; Yaghi, O. M. *Nat. Chem.* **2010**, *2*, 235−238.

(8) Van Humbeck, J. F.; McDonald, T. M.; Jing, X. F.; Wiers, B. M.; Zhu, G. S.; Long, J. R. *J. Am. Chem. Soc.* **2014**, *136*, 2432−2440.

(9) Kajiwara, T.; Higuchi, M.; Watanabe, D.; Higashimura, H.; Yamada, T.; Kitagawa, H. *Chem.—Eur. J.* **2014**, *20*, 15611−15617.

(10) (a) Kosower, E. M.; Cotter, J. L. *J. Am. Chem. Soc.* **1964**, *86*, 5524−5527. (b) Kaneko, M.; Motoyoshi, J.; Yamada, A. *Nature* **1980**, *285*, 468−470. (c) Bird, C. L. *Chem. Soc. Rev.* **1981**, *10*, 49−82. (d) Monk, P. M. S. *The Viologens: Physicochemical Properties, Synthesis and Applications of the Salts of 4,4′-bipyridine*; John Wiley & Sons: New York, 1998. (e) Porter, W. W.; Vaid, T. P. *J. Org. Chem.* **2005**, *70*, 5028−5035. (f) Yao, Q. X.; Pan, L.; Jin, X. H.; Li, J.; Ju, Z. F.; Zhang, J. *Chem.—Eur. J.* **2009**, *15*, 11890−11897. (g) Higuchi, M.; Nakamura, K.; Horike, S.; Hijikata, Y.; Yanai, N.; Fukushima, T.; Kim, J.; Kato, K.; Takata, M.; Watanabe, D.; Oshima, S.; Kitagawa, S. *Angew. Chem., Int. Ed.* **2012**, *124*, 8369−8372.

(11) (a) Jin, X. H.; Sun, J. K.; Xu, X. M.; Li, Z. H.; Zhang, J. *Chem. Commun.* **2010**, *46*, 4695−4697. (b) Sun, J. K.; Cai, L. X.; Chen, Y. J.;

DOI: 10.1021/acs.inorgchem.5b00023
Inorg. Chem. 2015, 54, 3456−3461

Li, Z. H.; Zhang, J. *Chem. Commun.* **2011**, *47*, 6870−6872. (c) Sun, J. K.; Jin, X. H.; Cai, L. X.; Zhang, J. *J. Mater. Chem.* **2011**, *21*, 17667−17672.
(12) (a) Sheldrick, G. M. *SHELXS97*; University of Göttingen, Germany, 1997. (b) Sheldrick, G. M. *SHELXL97*; University of Göttingen, Germany, 1997.
(13) Spek, A. L. *PLATON, A Multipurpose Crystallographic Tool*; Utrecht University: Utrecht, The Netherlands, 2010.
(14) Horike, S.; Shimomura, S.; Kitagawa, S. *Nat. Chem.* **2009**, *1*, 695−704.
(15) (a) Yao, Q. X.; Ju, Z. F.; Jin, X. H.; Zhang, J. *Inorg. Chem.* **2009**, *48*, 1266−1268. (b) Wu, J. B.; Yan, Y.; Liu, B. K.; Wang, X. L.; Li, J. Y.; Yu, J. H. *Chem. Commun.* **2013**, *49*, 4995−4997.
(16) Kaneko, M.; Katakura, N.; Harada, C.; Takei, Y.; Hoshino, M. *Chem. Commun.* **2005**, 3436−3438.
(17) (a) Seredych, M.; Bandosz, T. J. *J. Phys. Chem. C* **2007**, *111*, 15596−15604. (b) Petit, C.; Seredych, M.; Bandosz, T. J. *J. Mater. Chem.* **2009**, *19*, 9176−9185. (c) Bandosz, T. J.; Petit, C. *Adsorption* **2011**, *17*, 5−16.
(18) Furtado, A. M. B.; Liu, J.; Wang, Y.; LeVan, M. D. *J. Mater. Chem.* **2011**, *21*, 6698−6706.

DOI: 10.1021/acs.inorgchem.5b00023
Inorg. Chem. 2015, 54, 3456−3461